PNAS RESEARCH ARTICLE | NEUROSCIENCE

Stabilizing selection in an identified multisensory neuron in blind cavefish

Mercedes Hildebrandt[a], Mona Kotewitsch[a], Sabrina Kaupp[a], Sophia Salomon[a], Stefan Schuster[a], and Peter Machnik[a,1]

Edited by John Hildebrand, The University of Arizona, Tucson, AZ; received August 6, 2024; accepted October 17, 2024

The ability to follow the evolutionary trajectories of specific neuronal cell types has led to major insights into the evolution of the vertebrate brain. Here, we study how cave life in the Mexican tetra (*Astyanax mexicanus*) has affected an identified giant multisensory neuron, the Mauthner neuron (MN). Because this neuron is crucial in driving rapid escapes, the absence of predation risk in the cave forms predicts a massive reduction in this neuron. Moreover, the absence of functional eyes in the *A. mexicanus* Pachón form predicts an even stronger reduction in the cell's large ventral dendrite that receives visual inputs in sighted fish species. We succeeded in recording in vivo from this neuron in the blind cavefish and two surface tetra (*A. mexicanus* and *Astyanax aeneus*), which offers unique chances to simultaneously study evolutionary changes in morphology and function in this giant neuron. In contrast to the predictions, we find that cave life, while sufficient to remove vision, has neither affected the cell's morphology nor its functional properties. This specifically includes the cell's ventral dendrite. Furthermore, cave life did not increase the variance in morphological or functional features. Rather, variability in surface and cave forms was the same, which suggests a complex stabilizing selection in this neuron and a continued role of its ventral dendrite. We found that adult cavefish are potent predators that readily attack smaller fish. So, one of the largely unknown stabilizing factors could be using the MN in such attacks and, in the young fish, escaping them.

brain evolution | single neuron evolution | cavefish | neuronal cell type | environmental change

Significance

Comparing cave and surface forms of Mexican tetra allowed major insights into the evolutionary trajectory of numerous traits subsequent to a defined major environmental change. Here, we test specific hypotheses on how cave life should have affected the evolutionary trajectory of the largest neuron in the vertebrate brain, the renowned Mauthner neuron. The absence of predators and the loss of vision predict massive reductions in this neuron and a loss of its visual dendrite. However, while cave life has sufficed to remove functional eyes, all morphological and functional features of this neuron are conserved and subject to a complex and presently not understood stabilizing selection with a continued role of its ventral dendrite.

Our understanding of the evolution of vertebrate brains has largely profited from the ability to track individual cell types (1–6). However, how diverse selective pressures have shaped the evolutionary trajectory of morphological and functional features of individual neurons is challenging to assess (for example, ref. 7). To address this would require, first, detailed information on in vivo function in addition to detailed knowledge of morphology and network connectivity and, second, defined and massive changes in an important condition. In the present study, we bring the advantage of the Mauthner neuron (MN) (8, 9) to bear in Mexican cavefish, one of the most potent models to examine the course of evolution after a drastic environmental change (10–25). The giant MN is the largest and one of the few neurons of the vertebrate brain in which each cell can be identified individually (Fig. 1*A*). This neuron and its associated networks offer several attractive features and allow clear and testable predictions on how environmental changes should have affected the morphology and function of this neuron and its network connectivity. The features of the giant MN are shaped to its role in driving the rapid and powerful initial bending, the first stage of the so-called C-start that fish use to escape predators (Fig. 1*B*) (8, 9, 26, 27) or to strike at prey (Fig. 1*C*) (28, 29). For instance, networks exist to ensure that only one of the two MNs fires only one action potential (AP). When an AP is fired in the soma of one of the MNs, the AP rapidly runs down the large diameter MN axon to excite all trunk muscles on one side of the body almost simultaneously. The axons characteristically cross the midline (Fig. 1*A*) and activate (via motor neurons) muscles on the side contralateral to the soma position of the firing cell (Fig. 1 *B* and *C*). To drive an AP, the MN receives multisensory input (Fig. 1*A*). Its major dendrites are the ventral dendrite that receives input from the eyes (30) and the lateral dendrite that processes mechanosensory information forwarded by the ears and the lateral line organ (26, 31). In light of the extensive knowledge of the life of blind cavefish, the fate of the neuron would appear to be clear: first, because cavefish do not encounter predators (32) but also do not require rapid maneuvers to efficiently prey on other fish (33, 34), selective pressures on maintaining the large and presumably costly MNs should be relaxed and the neuron as well as its associated networks should be massively reduced or restructured to serve other functions. Second, in cavefish lacking functional eyes (i.e., lacking a functional retina),

Author affiliations: [a]Department of Animal Physiology, University of Bayreuth, Bayreuth 95440, Germany

Author contributions: S.Schuster and P.M. designed research; M.H., M.K., S.K., S.Salomon, and P.M. performed research; M.H., M.K., S.K., S. Salomon, S. Schuster, and P.M. analyzed data; and S.Schuster and P.M. wrote the paper.

The authors declare no competing interest.

This article is a PNAS Direct Submission.

[1]To whom correspondence may be addressed. Email: peter.machnik@uni-bayreuth.de.

This article contains supporting information online at https://www.pnas.org/lookup/suppl/doi:10.1073/pnas.2415854121/-/DCSupplemental.

Published November 18, 2024.

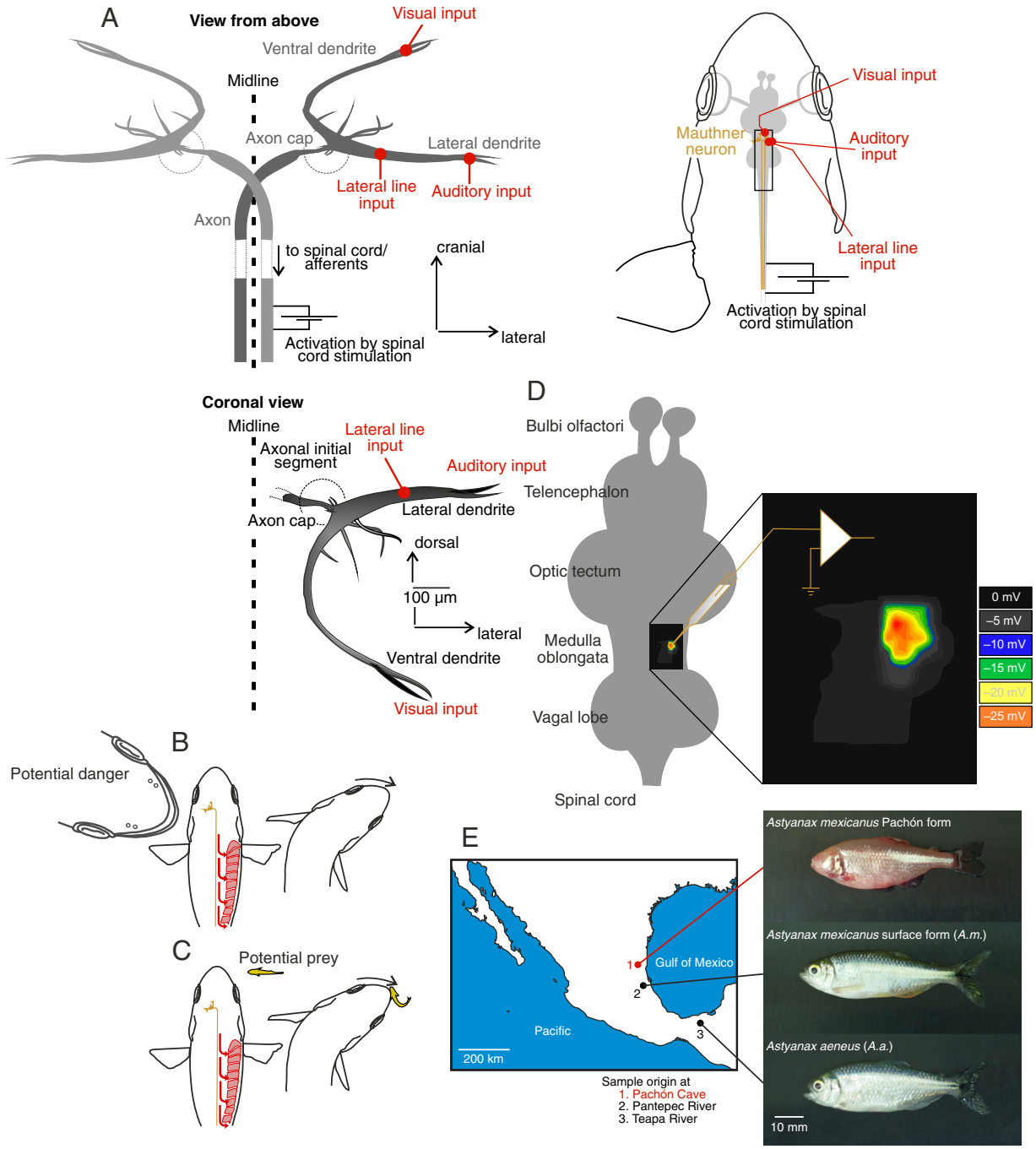

Fig. 1. Clear predictions of how cave life should have affected the evolutionary trajectory of the Mauthner neuron (MN). (*A*) The MN, the largest and presumably most costly neuron in the vertebrate brain, is an identified command neuron. If present, there are always only two MNs in the brain, one in the left and one in the right hemisphere of the medulla oblongata. The MNs integrate sensory information from all sensory systems to initiate a fast-start response if required. The sketch shows "typical" teleost MNs from above (*Below*: additional coronal view of the right MN). Note the two major dendrites, the lateral one (LD) and the ventral one (VD). The LD integrates information forwarded from the ears and from the lateral line organ. The VD integrates information forwarded from the eyes in sighted fish species. As indicated, the MN axon crosses midline in the medulla to contralaterally run down the entire spinal cord. (*B*) The MNs play a key role in the teleost fast-start escape performed in response to the sudden approach of a predator, and (*C*) have been suggested to play a role in the fast bending during prey capture behavior. The turns shown in the sketch would result from firing an AP by the left MN. This AP will rapidly run down the right body side and will cause almost simultaneous and thus forceful contraction of muscles on the right body side. (*D*) The MNs are deeply buried in the brain. In some fish, however, the MNs can be localized by a field potential that radiates from a structure called axon cap, whenever the MN fires an AP. In these fish, the cap surrounds the axon hillock of the MN. Hence, antidromic stimulation of the MN axon [as indicated in (*A*)] can be used in such fish to guide an electrode to the MN soma for in vivo intracellular recording and labeling. (*E*) For fish that lack predators, a strong reduction in the size of the large MN is expected as no rapid integration and conduction of an AP are needed to generate forceful contractions. Also, the existence of other structures important for MN function, including an axon cap, seems not required. Moreover, a loss of vision should lead to a loss or at least massive reduction in the VD. We test these predictions in the blind *A. mexicanus* Pachón form in comparison to the *A. mexicanus* surface form and the banded tetra (*A. aeneus*).

the ventral dendrite of their MNs would be predicted to be reduced or even absent (as reported in larvae of the blind Mexican tetra Pachón form (35). To test these predictions, we attempted to adapt (Fig. 1*D*) and establish techniques that would allow us in vivo intracellular recording and single-cell labeling in adult Mexican tetra cavefish of the blind Pachón form (*Astyanax mexicanus* Pachón form), the Mexican tetra surface form (*A.m.* = *A. mexicanus*), and the banded tetra (*A.a.* = *Astyanax aeneus*) (Fig. 1*E*).

Results and Discussion

Cave Life Had No Major Impact on the Physiological Hallmarks of the MN. The expected reduction of the cavefish MN could have meant the absence of an axon cap (Fig. 1*D*). However, we found that an axon cap is present in all three forms, including the blind cavefish. Applying electrical pulses to the spinal cord (in the area of the trunk) caused a negative field potential in the medulla of the cavefish. The field potential was of an all-or-nothing character, with fixed amplitude above a threshold stimulation strength in each recording position in the medulla (Fig. 2*A*). Amplitude depended on the recording position, and its gradient clearly reveals a single center in each of the two medullary hemispheres (Fig. 2 *B* and *C*). This is the hallmark feature of an axon cap that surrounds the MN axon hillock and its axonal initial segment in teleost fish (Fig. 1*A*) (36, 37). When the MN is activated, e.g., antidromically by spinal cord stimulation, a negative all-or-nothing field potential arises in the center of the axon cap (Fig. 1*D*) that can be used to guide a recording electrode to the soma of the MN (38). We therefore could show that the MN of the cavefish, and of both surface forms (Fig. 1*E*), has an axon cap. This important finding paves the way for localizing the MN in all three forms for in vivo intracellular recording.

An important physiological hallmark of a functional MN is that it responds with PSPs to a variety of sensory stimuli (Fig. 1*A*) (9). Therefore, we started our functional examination by examining whether sound pulses cause PSPs in the MN of all three forms. Using a standardized acoustic pulse caused PSPs in surface fish and in the blind cavefish (Fig. 2*D*), but PSP amplitude was systematically larger in the surface than in the cave form. PSP amplitude was 3.27 ± 0.39 mV in the cavefish (N = 11; 10 ≤ n ≤ 36 pulses), but 6.71 ± 0.44 mV in *A.m.* (N = 16; 5 ≤ n ≤ 40) and 7.34 ± 0.85 mV in *A.a.* (N = 14, 14 ≤ n ≤ 36) (one-way ANOVA: $P = 0.0002$, F = 11.17, $R^2 = 0.3703$; Tukey's test: cavefish vs. *A.m.*: $P = 0.0012$; cavefish vs. *A.a.*: $P = 0.0002$; *A.m.* vs. *A.a.*: $P = 0.7304$). PSP latency was 9.72 ± 0.26 ms in the cavefish, but shorter in the surface fish (*A.m.*: 8.06 ± 0.16 ms; *A.a.*: 8.04 ± 0.15 ms) (one-way ANOVA: $P < 0.0001$, F = 23.69, $R^2 = 0.5549$; Tukey's test: cavefish vs. *A.m.*: $P < 0.0001$; cavefish vs. *A.a.*: $P < 0.0001$; *A.m.* vs. *A.a.*: $P = 0.9979$). So, the MN of adult cavefish does receive acoustic information but less efficiently than the surface forms. Interestingly, the lower efficiency in the cavefish is not due to reduced hearing capacities. Hearing plays a significant role in the communication of both surface and cave tetras (40) and hearing sensitivity is similar in both (41, 42).

Visually induced PSPs could readily be recorded in the MNs of the two surface forms, but as expected not in the cavefish MNs (Fig. 2*D*). A visual PSP occurred 30.58 ± 1.51 ms (N = 16, 4 ≤ n ≤ 17) after our standardized light flash in *A.m.* (*A.a.* (N = 14, 3 ≤ n ≤ 16): 31.17 ± 1.46 ms) and had an amplitude of 1.42 ± 0.14 mV (*A.a.*: 1.95 ± 0.37 mV).

We next compared the shape and propagation of the AP by electrically stimulating the spinal cord 20 mm from the recording site in the MN soma (as indicated in Fig. 1*A*). All three forms showed one single AP in the soma a very short delay after spinal cord stimulation and 20 mm/delay gave the conduction speed of the MN axon in the three forms (Fig. 2*E*). Most notably is the finding that conduction speed is still high in the blind cavefish (N = 11; 79 ± 4 m s^{-1}), but lower than in the two surface forms (*A.m.* (N = 16): 95 ± 5 m s^{-1}; *A.a.* (N = 14): 101 ± 4 m s^{-1}; one-way ANOVA: $P = 0.0078$, F = 5.535, $R^2 = 0.2256$; Tukey's test: cavefish vs. *A.m.*: $P = 0.0433$; cavefish vs. *A.a.*: $P = 0.0070$; *A.m.* vs. *A.a.*: $P = 0.6544$). However, the shape of the AP and its amplitude revealed no significant differences between the cave and surface forms (cavefish: 29.3 ± 2.2 mV; *A.m.*: 31.2 ± 1.3 mV; *A.a.*: 30.1 ± 1.8 mV; one-way ANOVA: $P = 0.2975$, F = 0.2975, $R^2 = 0.0154$). The duration of the AP (measured at half-maximal amplitude) was longer in the cavefish (cavefish: 0.61 ± 0.03 ms; *A.m.*: 0.49 ± 0.01 ms; *A.a.*: 0.54 ± 0.02 ms; one-way ANOVA: $P = 0.0004$, F = 9.718, $R^2 = 0.3384$; Tukey's test: cavefish vs. *A.m.*: $P = 0.0002$; cavefish vs. *A.a.*: $P = 0.0303$; *A.m.* vs. *A.a.*: $P = 0.1854$) and the resting potential lower (cavefish: –82.1 ± 0.7 mV; *A.m.*: –77.5 ± 1.1 mV; *A.a.*: –77.7 ± 1.1 mV; one-way ANOVA: $P = 0.0067$, F = 5.722, $R^2 = 0.2315$; Tukey's test: cavefish vs. *A.m.*: $P = 0.0100$; cavefish vs. *A.a.*: $P = 0.0167$; *A.m.* vs. *A.a.*: $P = 0.9915$), but, taken together, blind cavefish retain a fully functional MN. The conduction speed of its axon, while lower than that of the surface forms, is still well in the range of typical teleost MNs. It is at least 5 to 10 times faster than that of the next rapidly conducting axon in the teleost spinal cord (43).

We additionally examined a circuit property, feedback inhibition, that plays a key role in the function of the MN (36, 39, 44). Interestingly, this property seems not affected by cave life. To examine feedback inhibition, a second MN AP is elicited by electrical spinal cord stimulation a defined interval after the first AP. The reduction in amplitude of the second AP is a good measure of the strength of the inhibitory network effects that have been triggered by the first AP (45). Feedback inhibition is present in the surface forms as well as in the cavefish, has similarly long decay times, lasts over 30 ms in all the three forms (Fig. 2*F*), and compares well with properties found in other teleost fish (44). In summary, apart from the absence of visual PSPs, cave life has caused surprisingly little deficits in the basic physiological properties of the MN.

Cave Life Had No Major Effect on the Morphology of the MN. Using the field potential to localize the MN in the hindbrain of the blind cavefish and the two surface forms allowed us also to intracellularly stain the MNs of adult fish which is the basis for a detailed analysis of the cell's anatomy. Surprisingly, also all morphological features of the MNs did not differ between the cave and surface forms in any of the predicted ways. Fig. 3*A* illustrates this. It shows for length and diameter of the two major dendrites the two extreme examples found within each of the three forms. All forms exhibit a lateral and a ventral dendrite, a large soma, and various smaller dendrites. In contrast to the prediction and its apparent absence in the larva of this form (35), the adult cavefish of the Mexican tetra Pachón form still retained a fully developed ventral dendrite that also was equally variable across cave individuals than it was across the surface individuals (Fig. 3*A*). It has been demonstrated that Mexican tetra cavefish still retain a surprisingly intact optic tectum (46) and so the ventral dendrite is likely processing the remaining nonvisual inputs from the tectum. It is also likely that the massively increased mechanosensory afferent supply in cavefish (12, 19, 22) took over at least parts of the ventral dendrite, since the lateral dendrite is not, as it would otherwise be expected, increased in area in line with the increase in mechanosensory input. It is not easy to account for the absence of a notable ventral dendrite in the Pachón cavefish larva, as concluded from confocal images (35), but a specifically slow growth rate in the cavefish ventral dendrite might be a plausible explanation. The conclusion that a ventral dendrite is absent in adult cavefish, based on confocal images in larva after retrograde labeling, however, clearly is no longer tenable in view of our findings. Although the ventral dendrite has for some reason not been detected in the larva (35), we can show from intracellular MN labeling that in adult cavefish of the Pachón form the ventral dendrite is not only fully present but is even subject to stabilizing selection.

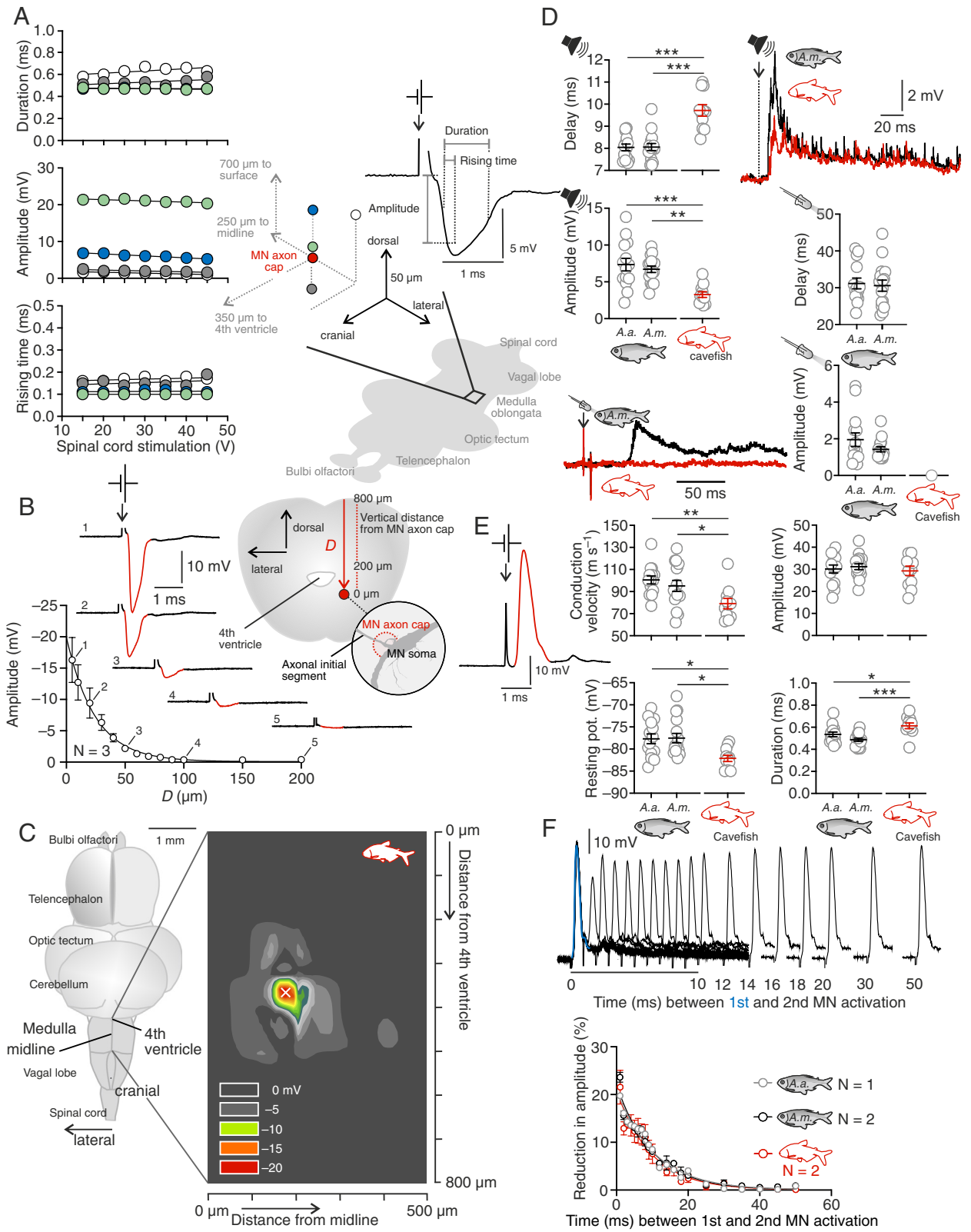

Fig. 2. Intracellular recordings in the MN of cavefish reveal surprisingly few changes relative to surface forms. (*A*–*C*) Blind cavefish still have a so-called axon cap that is crucial for localizing the MN for intracellular recording and staining. (*A*) Spinal cord stimulation causes an all-or-nothing field potential. (*B*) Example of how its amplitude changes during a direct vertical approach to the axon cap (*D* = distance from axon cap). (*C*) Field potential gradient in the horizontal plane in the right medullary hemisphere for one of the cavefish. This gradient reliably allows localizing the MN. (*D*) The MN of cavefish and surface fish responds with similarly shaped postsynaptic potentials (PSPs) to acoustic stimuli, but cavefish PSPs have lower amplitude and longer delay. Light flash stimuli elicit PSPs of similar amplitude and delay in the surface forms. (*E*) Time course and amplitude of the AP is similar in all forms, but it travels slightly slower in the cavefish. (*F*) Evidence for fully functional feedback inhibition in blind cavefish. This hallmark of MN network function ensures efficient fast starts (e.g., ref. 39) and has the same time course and strength across all forms. It is revealed by probing the reduction in amplitude of a 2nd AP a short interval after a preceding one. One, two, three asterisks indicate $P \leq 0.05$, $P \leq 0.01$, or $P \leq 0.001$, respectively.

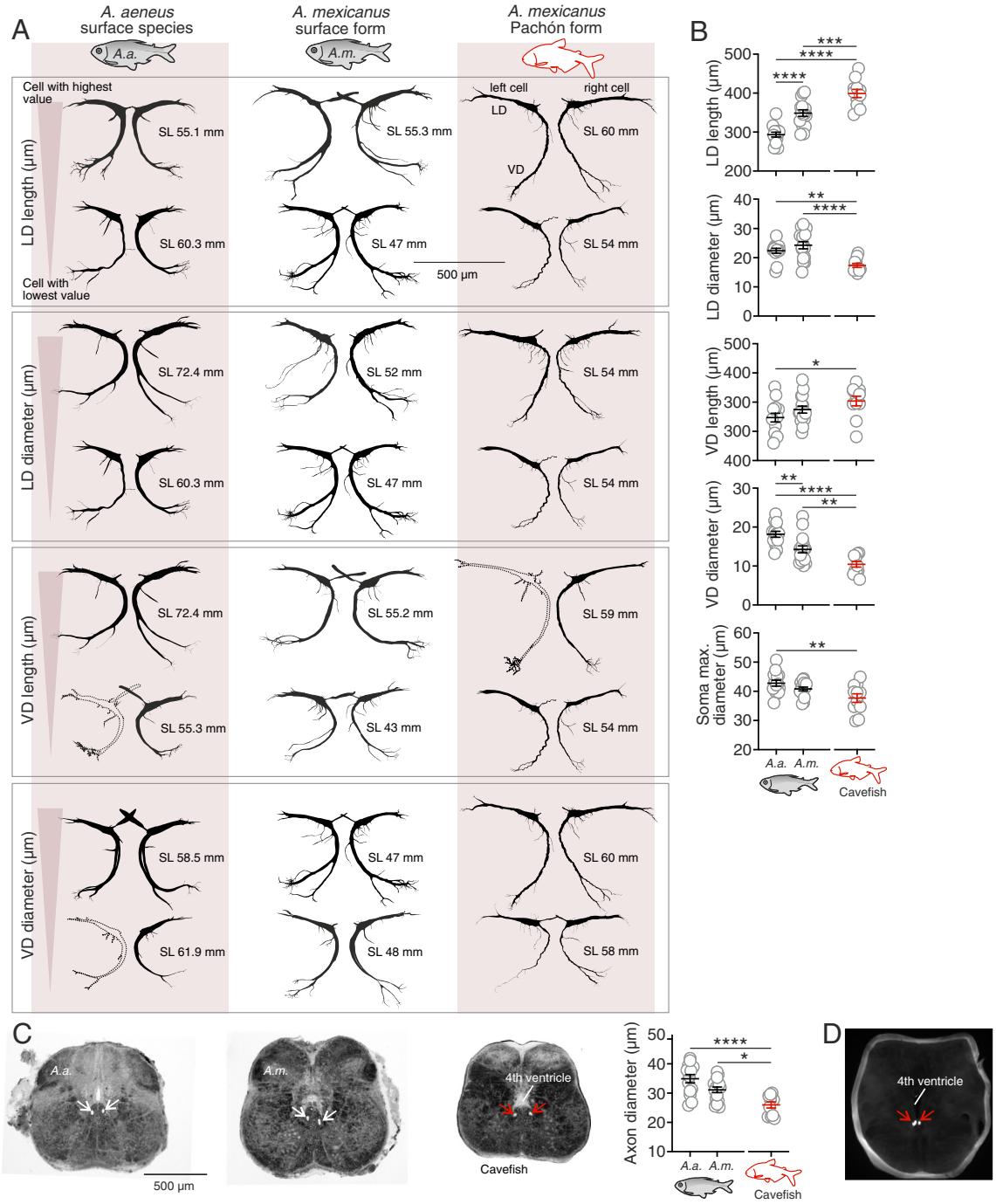

Fig. 3. Cave life has not changed the morphology of the MN in adult blind cavefish. (*A*) We were able to intracellularly label at least one of the two MN in all examined fish (N = 14 *A.a.*, N = 16 *A.m.*, and N = 11 cavefish). MNs that were labeled are shown in black, in some cases, the second cell could not be labeled (indicated as unfilled cells). To indicate the degree in variability in the lateral (LD) and ventral (VD) dendrite, the cell with the highest and lowest value is shown for each of the parameters analyzed and for each group of fish (fish size is given as standard length, SL). (*B*) Differences in the morphological properties of the MN occur not only between the cavefish and the surface forms but also between the surface forms. (*C*) Exemplary unstained coronal slices of the spinal cord to show that the large-diameter MN axons can be easily identified even in unstained sections. Axon diameter (determined at the spinal cord/brain junction) was large in all forms but significantly smaller in the cavefish. (*D*) Exemplarily coronal slice of the spinal cord after tracer injection into the MN cell bodies to demonstrate that the structures pointed in (*C*) are indeed the MN axons. LD: lateral dendrite, VD: ventral dendrite; one, two, three, four asterisks indicate $P \leq 0.05$, $P \leq 0.01$, $P \leq 0.001$, or $P < 0.0001$, respectively.

For a quantitative analysis of key morphological features, we made detailed measurements. The major differences are summarized in *SI Appendix*, Table S1. In the cavefish, the maximum diameter of the MN soma was 37.7 ± 1.5 µm (N = 11) (*A.m.* (N = 16): 40.8 ± 0.6 µm; *A.a.* (N = 14): 42.8 ± 1.0 µm). Its lateral dendrite had a length of 399.2 ± 10.5 µm (*A.m.*: 348.7 ± 8.3 µm; *A.a.*: 293.5 ± 6.1 µm), and a diameter of 17.4 ± 0.7 µm (*A.m.*: 24.3 ± 1.2 µm; *A.a.*: 22.4 ± 0.8 µm). The ventral dendrite had a length of 603.9 ± 16.4 µm (*A.m.*: 574.4 ± 12.0 µm; *A.a.*: 547.0 ± 14.9 µm), and a diameter of 10.4 ± 0.7 µm (*A.m.*: 14.3 ± 0.9 µm; *A.a.*: 18.2 ± 0.8 µm). Maximum soma diameter, dendritic lengths, and diameters reveal significant differences across the three forms (Fig. 3*B*; one-way ANOVA: $P \leq 0.0360$, $F \geq 3.633$, $R^2 \geq 0.1605$), however, without any direct effect that could easily be attributed to cave life or to the absence of functional eyes. For instance, the lateral dendrite in the cavefish is longer than in *A.m.*, but it also has a lesser

diameter. Furthermore, similar differences can even be found in the two surface forms (Fig. 3*B* and *SI Appendix*, Table S1), suggesting that other factors than cave life are more important in shaping these morphological differences.

We next analyzed the MN axons in the three forms. To study them, we prepared coronal slices from the medulla into the spinal cord. The large-diameter MN axons of both cave and surface fish can easily be spotted in every coronal slice (Fig. 3*C*). That these axons are indeed the MN axons is confirmed by comparing them with fluorescence in axons of MNs that had been injected tracer to the MN soma (Fig. 3*D*). Following their course showed that in all three forms the axons cross the midline in the medulla (*SI Appendix*, Fig. S1), as is typical for MNs (47). So also this feature is conserved in the cavefish. Most importantly, the diameter of the MN axons was large in all forms. We determined MN axon diameter at the transition from the spinal cord to the brain from five consecutive coronal slices. It was 26.0 ± 1.0 µm in the cavefish (N = 11), 31.1 ± 1.0 µm in *A.m.* (N = 16) and 34.9 ± 1.4 µm in *A.a.* (N = 14) (Fig. 3*C*; one-way ANOVA: $P < 0.0001$, F = 13.33, $R^2 = 0.4124$; Tukey's test: cavefish vs. *A.m.*: $P = 0.0110$; cavefish vs. *A.a.*: $P < 0.0001$; *A.m.* vs. *A.a.*: $P = 0.0535$). The axon of the cavefish MN has a smaller diameter than that of the surface forms. However, in all three forms, the MN axon is at least 5 to 10 times larger in diameter than the largest other axons in the teleost spinal cord (43).

Evidence for Stabilizing Selection in the Cavefish MN. So far, we have demonstrated that in contrast to the predictions, the cavefish MN has not been reduced in any major way. It shares all functional and morphological characteristics with the surface forms that we have studied for direct comparison. Specifically, despite the absence of functional eyes, the ventral dendrite of the cavefish MN has clearly not been reduced and is, surprisingly, similar to that of the sighted forms. However, this analysis still misses one important aspect in which the drastic change in crucial selection factors, the absence of predators and of light, could also have acted: an increased variability in some of the morphological and functional characteristics. For example, while the average size of the ventral dendrite is unchanged, the interindividual variation around this average should be far larger in the cavefish, compared to the variation in the surface forms.

To examine this prediction, we analyzed the degree of interindividual variation in functional (Fig. 2) and morphological (Fig. 3) characteristics of the MNs of cavefish and the two surface forms. Fig. 4 reports the findings of this analysis. For all functional characteristics we had examined, the coefficients of variation were comparable for cavefish and the two surface forms (Fig. 4 *A* and *B*). Against the predicted effect, the physiological properties of the MN did not show increased variability. But the same also held for the morphological characteristics (Fig. 4*C* and *SI Appendix*, Table S2). Also, here, we failed to see the predicted higher variation in the cavefish compared to the surface forms.

On average, the coefficient of variation of the physiological features was 17.7% for the cavefish MN (*A.m.*: 15.1%; *A.a.*: 17.8%) and 13.4% for morphological features of the cavefish MN (*A.m.*: 13.9%; *A.a.*: 11.3%). For the ventral dendrite, coefficients of variation were 9.0% for length and 23.2% for diameter. These values are strikingly similar in *A.m.* (8.3% and 24.9%, respectively) and *A.a.* (10.2% and 15.8%, respectively).

Taken together, interindividual variability in the MN is not significantly different across the three forms (Fig. 4*D*; repeated measures ANOVA: $P = 0.7446$, F = 0.2989, $R^2 = 0.0265$). This

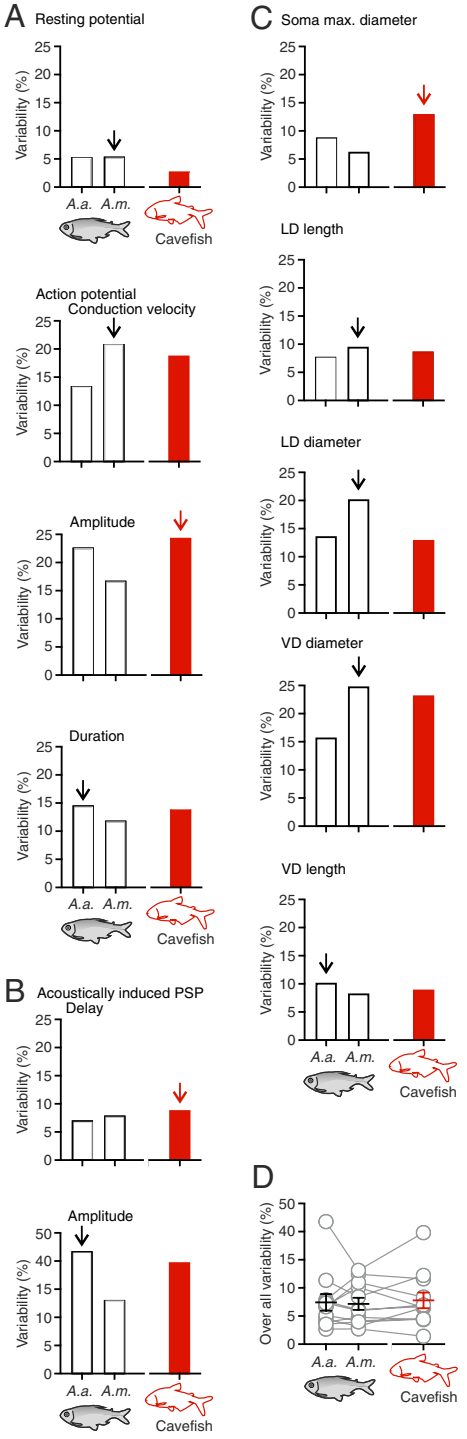

Fig. 4. Evidence for stabilizing selection in the MN in the blind cavefish. Diminished selective pressures should cause increased variability in some properties of the cavefish MN, such as the length and diameter of its ventral dendrite (VD). However, variability is not largest in cavefish. Rather, coefficients of variation for the physiological properties (Fig. 2 *D* and *E*) and for morphological properties (Fig. 3 *A* and *B*) are similar in cavefish and surface forms. (*A*) shows the coefficient of variation for the resting potential and properties of the AP of the MN (N = 14 *A.a.*, N = 16 *A.m.*, and N = 11 cavefish), and (*B*) for properties of the acoustically induced PSPs in the MN. (*C*) shows the variation in morphological properties. Note that highest variability in length and diameter of the VD is found in the surface forms. In each case, an arrow highlights the largest coefficient of variation. (*D*) The overall variability does not significantly differ between cavefish and surface forms (repeated measures ANOVA: $P = 0.7446$, F = 0.2989, $R^2 = 0.0265$). Open circles show variability of specific factors (*A*–*C*), each connected by a line. Means ± SEM are indicated across all factors.

demonstrates, contrary to the predictions, that some stabilizing selection still acts on the cavefish MN. Within the timespan that sufficed to remove functional eyes and to change many other key physiological features, the MN was kept and not even its variability has been increased. This is the most massive failure for a prediction on the evolutionary fate of a neuron and could not be more obvious and easier to test quantitatively.

Adult Cavefish Rapidly Strike at and Devour Smaller Fish. Clearly, our findings on both physiology and morphology of the MN are not only completely at odds with all predictions but even suggest stabilizing selection of all morphological and physiological features of the MN in the Mexican cavefish. Although the adults are assumed to feed exclusively on organic material washed into the caves and the biofilm growing on it (32–34) we examined a possibility that might contribute to the otherwise unknown selection factors that stabilize the features of the MN. Because cannibalism is not uncommon in other tetras (48), we tested whether the adult cavefish would be able to efficiently strike at and devour smaller fish. Indeed, we recorded several instances in which adults attacked and ate smaller fish. Fig. 5*A* shows two examples of attacks on smaller fish that were recorded with digital high-speed video. In both attacks, the smaller fish was later eaten. Note that in both examples the adult fish responds with a rapid C-shaped bend to the passing smaller fish before biting into it (Fig. 5*A*). This was seen in 6 of 10 attacks recorded with high-speed video and the bending duration was typically of 20 ms duration. This is noteworthy, because this is in the range of bending duration of MN-induced C-starts and because MN activity has been recorded during prey capture or has been suggested to play a role in prey capture from kinematics in other teleost fish (28, 29). The recordings of Fig. 5*A* suggest two potential roles the MN might still play in blind cavefish: in the young fish, they might be needed to efficiently escape the attacks of adult conspecifics. In the older fish, they might potentially be employed to drive rapid strikes at smaller fish.

To estimate the risk of being attacked by an adult, we monitored groups with one adult cavefish and 10 smaller fish of a set standard size SL from 4.3 ± 0.1 mm to 15.8 ± 0.1 mm). Additionally, we also tested the most vulnerable [=physically smallest (SL ≤ 4.3 mm)] group of small fish with dark-adapted adult *A. mexicanus* surface fish to compare their hunting success with that of the cavefish. With a cavefish nearby, all smaller fish faced the risk of becoming prey, but the risk decreased exponentially with increasing size [model: y = 73.54*exp(–3.95*x); R^2 = 0.99] from 14% in fish with a SL of 4.3 mm to 0.5% in fish with a SL greater than 15 mm (Fig. 5*B*). These observations were made in the dark. Tested under the same conditions, the surface fish were not half as effective at catching smaller fish as the cavefish (Fig. 5*B*; Mann–Whitney test, P = 0.0311). Results in the cavefish also hold under light conditions (Fig. 5*C*; paired t test: t = 0.3224, df = 4, P = 0.7633), so we were able to document the attacks more closely by filming groups of N = 20 smaller fish and three adult cavefish in a tank (frame rate: 60 Hz) for 60 min. Physical contact between adult and small fish was frequent [50.3 ± 8.0 contacts in 60 min/adult individual (N = 15; 5 independent groups)]. Attempts to snap at one of the smaller fish were observed regularly (Fig. 5*D*; 4.9 ± 0.9 snaps in 60 min/adult individual), but snaps were seen only after a prior contact in the front half of the adult fish's body. Several smaller fish were sucked in and eaten (Movies S1 and S2).

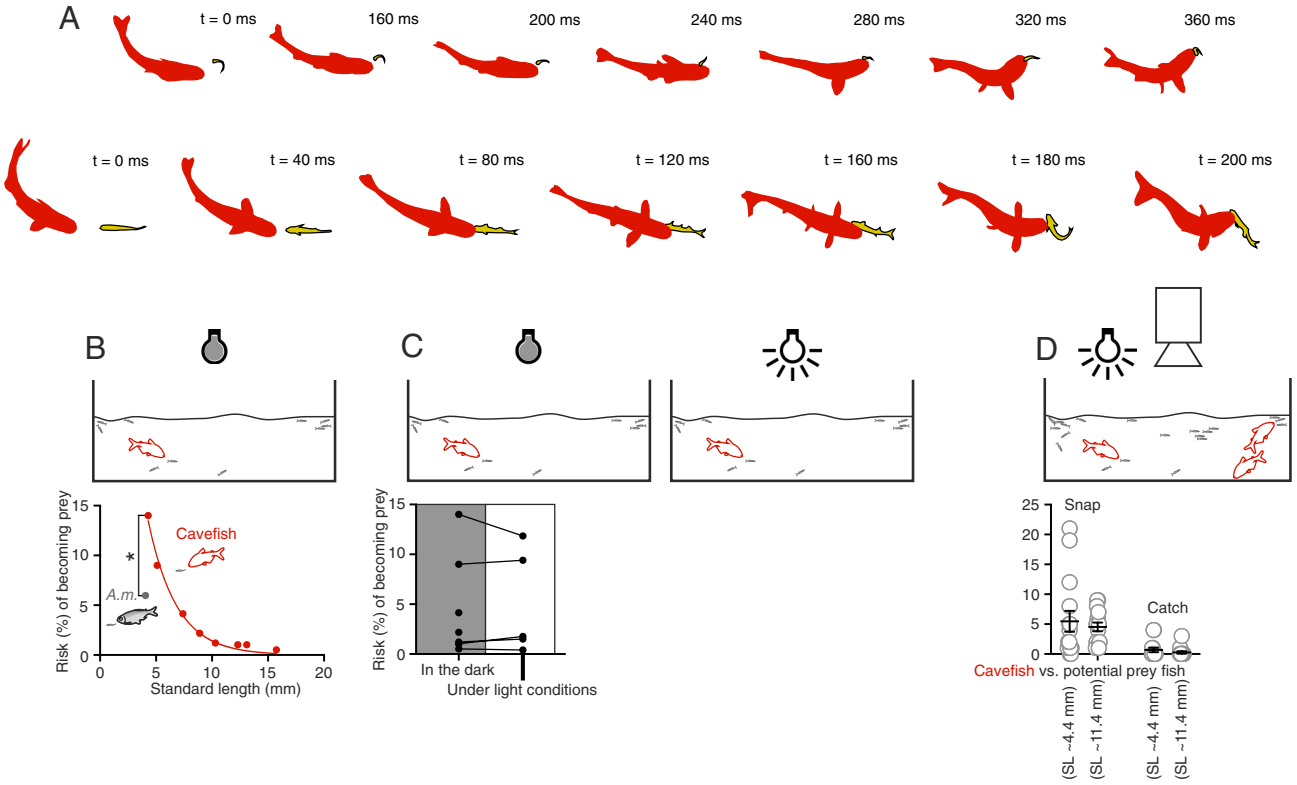

Fig. 5. Powerful attack behavior of adult cavefish could be one of the stabilizing factors in the evolution of the cavefish MN. (*A*) Two examples of how an adult cavefish catches a smaller fish. Prey fish were subsequently devoured. Note C-bend of the adult fish before the attack. (*B*) The probability of falling prey to adult cavefish decreases with increasing size (solid curve: exponential decline) but is still nonzero for fish sized 1.5 cm. In comparison to dark-adapted surface fish of *A. mexicanus*, the cave form is more effective at catching small fish in the dark. (*C*) Facing an adult cavefish, predation risk is similar under light and dark conditions. (*D*) Analysis of 60 min video recordings made in 15 adult cavefish to show that attacks on smaller fish (SL as indicated) are common and that the adults readily prey on the smaller fish if these fail to escape. One asterisk indicates $P \leq 0.05$.

Conclusion

We have shown that it is possible to bring the unique advantages of the MN to bear in one of the best systems to examine the course of evolution of a neuronal cell type after a drastic environmental change. The lack of predators and intact eyes in cavefish but not in the surface-dwelling relatives yields particularly clear and experimentally testable predictions on the evolutionary trajectory of this neuron. The most striking aspect, and potentially warning for the study of the evolution of neuronal cell types, is how clearly all predictions failed. Within the time frame that sufficed to reduce the eyes and to adapt key physiological features (10–25), this one multisensory interneuron changed none of its features and not even the variability across individuals is different from the surface forms. The selective factors that act to so efficiently stabilize all features of the MN are presently unknown. Clearly, the input to the ventral dendrite must have shifted to other inputs. These could still be processed in the optic tectum of cavefish (46). The ventral dendrite could, for instance, receive mechanosensory inputs, which are massively increased in cavefish compared to the surface form (12, 19, 22). Mechanosensory inputs play an important role in prey capture in larval cavefish (12, 22) and apparently do so in adults as well: our observation of intraspecific predation could explain to some extent the functional stabilization of the MN in the adult cavefish and the idea of a takeover of the ventral dendrite by mechanosensory inputs would explain its morphological stabilization. However, because of the magnitude of stabilization that we found, we suggest that a suite of additional, perhaps developmental, factors are also at play. Studies on escape response networks in Diptera indicate that once evolved, the main players in a highly constrained neuronal network are extraordinarily stabilized during evolution (49, 50). The expectation in fish therefore might also be that a neuronal ground pattern ubiquitous to this clade should be extraordinarily robust irrespective of a broad range of ecologies. Our results would support this idea. So, our study in a case that should be particularly clear and testable demonstrates that predicting the evolution of neuronal cell types in the vertebrate brain can be strikingly far from obvious.

Materials and Methods

Animals. For electrophysiological recordings and labeling of the MN, we used N = 11 *A. mexicanus* of the hypogean Pachón form (Pachón cave, Mexico; provided by Horst Wilkens, CeNak, University of Hamburg, Hamburg, Germany), and N = 16 epigean *A. mexicanus* from Pantepec River (Tuxpan River basin, Mexico; obtained from the specialist retailer Thomas Tillmann (Duisburg, Germany)). In addition, we used N = 14 epigean *Astyanax aeneus* from Teapa River (State of Tabasco, Mexico; also provided by Horst Wilkens). The fish were of both sexes. Sex was identified after recording. The cavefish had a SL of 57.3 ± 0.9 mm (ranging from 53.0 to 61.0 mm). They were the offspring of fish collected from Pachón cave by Horst Wilkens in 1971, and all were of the type shown in Fig. 1*E*. Without pigmented eyes and without body pigmentation, they represent the natural Pachón population with the respective genetical background before the introgression event in the 1980 s in connection with a pipeline project (19, 51–53). From that information, additional direct analyses of the fish's genetical background of Wilken's fish (19, 52) and our results (Fig. 2*D*), we exclude the possibility that the fish used had a cave/river hybrid background. In the epigean form of *A. mexicanus,* SL was 51.3 ± 1.4 mm (ranging from 43.0 to 59.8 mm), and 61.3 ± 1.5 mm (ranging from 53.8 to 72.4 mm) in *A. aeneus*. Prior to the experiments, the fish were kept in population-specific groups for at least 24 wk in several glass tanks (120 × 50 × 50 cm) with fresh water (water conductivity: 0.3 mS cm^{-1}; water temperature: 23 °C). To match natural conditions, the epigean forms were kept at a 12:12 h light/dark photoperiod. The cave form was kept in the dark. For MN recording and labeling, only healthy fish were selected by evaluating behavior (swimming, foraging) and external body conditions. Only fish without skin changes, injuries, and torn fins were used in the experiments. To assay predation risk, we used zebrafish (*Danio rerio*) as prey. Their SL (age) ranged from 4.1 ± 0.1 mm (2 wk) to 15.8 ± 0.1 mm (20 wk). Keeping conditions and performed procedures were in accordance with all relevant guidelines of the German Animal Welfare Act and explicitly approved by the Council of State.

Anesthesia and Surgical Procedure. Surgical intervention is required to access the MN for in vivo intracellular recording and tracer injection. Prior to surgery, the experimental fish were transferred to a small anesthetization tank. Anesthesia was achieved by adding 400 mg L^{-1} 2-phenoxyethanol (Merck KGaA, Darmstadt, Germany) (54). Within 10 min, all fish stopped swimming and lost equilibrium. When the experimental fish lost responsiveness to touch and handling, it was placed in the electrophysiological setup. Artificial respiration was established by running aerated water over the fish's gills via a tube in the fish's mouth. Respiration water also contained the same concentration of 2-phenoxyethanol as was used to induce anesthesia. It was delivered to the fish from a respiration water tank using a suitably adjusted pump (EHEIM universal 300; EHEIM GmbH & Co. KG, Deizisau, Germany; regular power: 300 L h^{-1}, adjusted to 3.0 L h^{-1}).

In teleost fish, the two MNs are located in the medulla oblongata, which is part of the vertebrate hindbrain. To get access, we exposed the brain from above from the optic tectum to the vagal lobe. The cerebellum was lifted upward and cranially to expose the medulla. Meninges covering the medulla were removed. A piece of 1 mm of the spinal column was exposed in the area of the trunk to place a custom-made bipolar stimulation electrode. The distance between the stimulation site and the recording site in the MN soma was 20 mm. Via the stimulation electrode, electrical pulses could be applied to cause strong twitching of the experimental fish and thus to confirm activation of the MN in the spinal cord. Subsequently, we immobilized the experimental fish for MN recording and labeling by intramuscular injection of d-tubocurarine (Sigma-Aldrich T2379; Merck KGaA, Darmstadt, Germany; 1 μg g^{-1} body weight). After finishing recordings and tracer injection, the brain was fixated (4% paraformaldehyde (PFA) solution) and extracted for further processing.

Electrophysiological Measurements. We found that the MN of cavefish exhibits an axon cap. This allowed us to use established techniques to localize the MN in the medulla and to identify it in vivo (38, 55). For that, we used a bridge-mode amplifier (BA-01X, npi electronic GmbH, Tamm, Germany) in current-clamp mode. Electrodes used for recording were pulled from glass capillaries (G-3; Narishige International Ltd., London, UK). To get a sharp electrode, the tip was broken. Filled with 5 mol L^{-1} potassium acetate, electrodes had a resistance between 4 and 7 MΩ. To position the electrode in the MN soma, we used a motorized micromanipulator (MP-285; Sutter Instruments, Novato, CA). The reference electrode was placed stationary in muscle tissue. Recordings were filtered (Hum Bug Noise Eliminator; Quest Scientific, North Vancouver, BC, Canada) and digitized (A/D converter Micro1401; Cambridge Electronic Design Limited, Cambridge, UK) at 50 kHz. For further processing and analysis, we used the acquisition software package Spike2 (version 6; Cambridge Electronic Design Limited, Cambridge, UK) and custom-made software written in Python.

To activate the MN antidromically (by applying electrical pulses to the spinal cord), we used a constant-voltage isolated stimulator (DS2A2 – Mk.II; Digitimer Ltd., Hertfordshire, UK) and a custom-made bipolar stimulation electrode that was positioned on the spinal cord. The stimulator delivered electrical rectangular pulses of 10 μs duration and variable amplitude. Pulse amplitude was determined in each experiment by decreasing the amplitude of the stimulation pulse until it did not activate the MN anymore. Then it was increased again to be 10 V above activation threshold. For acoustic stimulation, we used an active loudspeaker (The box pro Achat 115 MA; Thomann GmbH, Burgebrach, Germany). The loudspeaker generated a short acoustical broadband pulse (duration: 1 ms; frequency distribution from 25 to 1,000 Hz; peak amplitude at 300 Hz) with a sound pressure level (SPL) of 145 dB re 1 μPa. We measured SPL under water at the position of the fish in the recording chamber with a hydrophone (Type 8106; Brüel & Kjær, Nærum, Denmark). For visual stimulation, we used a light flash (7 ms in duration) elicited by a light-emitting diode (LED; RS Components GmbH, Mörfelden-Walldorf, Germany). The LED was positioned directly in front of the ipsilateral eye or in front of the ipsilateral eye cavity in eyeless cavefish. LED peak radiation at 569 nm was 700 μW m^{-2} nm^{-1} and the width at 100 μW m^{-2} nm^{-1} was 56 nm (range: 543 to 599 nm).

To generate the heat map shown in Fig. 2*C*, we activated the MNs antidromically. The recording electrode was moved vertically into the brain and the field

potential amplitude measured during lowering: it always increased until a maximum was reached. When the electrode was moved deeper into the brain, the amplitude decreased again. By lowering and lifting the recording electrode in a particular horizontal recording position, the local maximum for that position could be determined. For the heat map, we took 94 sampling points in the entire right medullary hemisphere. Distance between recording positions ranged from 10 to 100 μm depending on the steepness of the gradient of the field potential.

To determine the effect of feedback inhibition shown in Fig. 2*F*, we elicited a second AP a defined short interval after the first one by electrical spinal cord stimulation. When feedback inhibition is present, the first AP would activate it. The reduction in amplitude of the second AP then is a good measure of its strength and impact (36, 44, 45).

MN Labeling. For MN labeling, the electrode placed in the MN was filled with Neurobiotin™ tracer (VEC-SP-1120-20; BIOZOL Diagnostica, Eching, Germany; solved in 1 mol L^{-1} potassium chloride). The tracer was injected into the cell iontophoretically (55, 56). To exclude the possibility that we evaluate morphological features of damaged cells, we continued processing after tracer injection only in cells that i) still showed a postsynaptic potential after acoustic stimulation and ii) still fired an AP when stimulated antidromically. If so, the brain and spinal cord were fixated (4% PFA solution at 4 °C), extracted from the skull, and sliced (40 to 70 μm-coronal slices) by using a vibrational microtome (VT1200 S, Leica Microsystems, Wetzlar, Germany). The spinal cord was sliced in 40 μm-coronal slices from caudal to cranial. When macrostructures indicated that we have reached the brain, we took five consecutive 40 μm-brain slices, in which we determined the diameter of the two MN axons directly after slicing under wet conditions. Then, we took 70 μm-brain slices until we definitely passed the position of the MN cell bodies in the medulla, that is until macrostructures indicated that the entire medulla had been sliced. The brain slices were washed in PBS and incubated with Streptavidin-Cy3 (Sigma-Aldrich) in PBX (PBS + 0.3% Triton™ X-100; Sigma-Aldrich). Streptavidin specifically binds to the Neurobiotin™ tracer (57). The brain slices then were washed again, dehydrated by using increasing alcohol concentrations (from 30 to 99%), placed on microscope slides, cleared by using methyl salicylate (Merck KGaA, Darmstadt, Germany), and covered by Entellan™ (Merck KGaA) and a coverslip. Subsequently, we examined the slices using a fluorescence optical microscope (Axio Scope.A1, Carl Zeiss Microscopy, Jena, Germany). If parts of a fluorescent cell were found in a brain slice, we made size-scaled photos by using an adjusted digital microscope camera. The 2D-reconstructions of the cells were made in CorelDraw 2021 (version 23.1.0.389; Corel Corporation, Ottawa, Ontario, Canada) and cell parameters were determined in Fiji (version 2.3.0/1.53f; NIH, Bethesda, MD).

Behavioral Testing. To estimate the risk of falling prey to an adult cavefish, we placed an adult cavefish in a tank (320 × 140 × 125 mm) together with 10 smaller fish of a specific size/age [SL from 4.3 ± 0.1 mm (2 wk old) to 15.8 ± 0.1 mm (20 wk old)]. Experiments were run in the dark. After 60 min, we removed the adult cavefish and then counted the remaining smaller fish. We did so in N = 10 independent groups for each size/age group of smaller fish. To compare effectiveness of catching smaller fish, we additionally used N = 20 dark-adapted *A. mexicanus* of the surface form with the most vulnerable (=physically smallest) group of smaller fish. Just as with the cavefish, the adult surface fish were placed with 10 smaller fish (SL 4.1 ± 0.1 mm) in a tank for 60 min in the dark. To determine whether the performance differs under light conditions in the cavefish, we also tested the same cavefish with the light switched on for some of the size/age groups of smaller fish. At least 2 d lay between the tests. Half of the animals were first tested in the light, the other half in the dark.

To directly document the attacks, we placed three adult cavefish in a tank (320 × 140 × 125 mm) together with 20 smaller fish and filmed them for 60 min continuously with a digital camera (either Sony α6300 or Olympus OM-D E-M10 III; frame rate: 60 Hz). In addition, we filmed attacks with a highspeed camera (NAC HotShot 2300CC; frame rate: 250 or 500 Hz). We did this in groups where all the smaller fish were the same age [either 2 (SL 4.4 ± 0.1 mm) or 10 to 12 wk (SL 11.4 ± 0.7 mm)] or with mixed groups of smaller fish.

Statistics and Reproducibility. Statistical analyses were run using Prism 8 (version 8.4.3 (471) for macOS; GraphPad Software, Inc., La Jolla, CA, USA) and performed two-tailed with $\alpha = 0.05$. Averages are given as mean ± SEM. N denotes the number of animal samples, and n the number of measurements per animal. When data from animals were pooled, we never used the measurement repetitions (n) taken from the individual animals, but a single averaged value for each animal. To test whether data are distributed normally (Gaussian), we used the Shapiro–Wilk test. When data were normally distributed, we used a parametric test design, otherwise a nonparametric one.

Data, Materials, and Software Availability. All study data are included in the article and/or supporting information.

ACKNOWLEDGMENTS. We thank Horst Wilkens and Thomas Tillmann for providing fish and Wolfram Schulze for writing software. We are grateful to Daniel Konn-Vetterlein, Antje Halwas, Nicholas Jones, Simon Goddemeier, Benedikt Maric, Susanne Proschke, and Elena Köstner for help, the three anonymous peer reviewers for many helpful and constructive comments, and Thomas Preuss and Donald S. Faber for introducing us to the art of Mauthner neuron recording.

1. R. G. Northcutt, Understanding vertebrate brain evolution. *Integ. Comp. Biol.* **42**, 743–756 (2002).
2. L. A. Krubitzer, A. M. H. Seelke, Cortical evolution in mammals: The bane and beauty of phenotypic variability. *Proc. Natl. Acad. Sci. U.S.A.* **109**, 10647–10654 (2012).
3. F. Sugahara, Y. Murakami, J. Pascual-Anaya, S. Kuratani, Reconstructing the ancestral vertebrate brain. *Dev. Growth Differ.* **59**, 163–174 (2017).
4. M. A. Tosches *et al.*, Evolution of pallium, hippocampus, and cortical cell types revealed by single-cell transcriptomics in reptiles. *Science* **360**, 881–888 (2018).
5. M. A. Tosches, G. Laurent, Evolution of neuronal identity in the cerebral cortex. *Curr. Opin. Neurobiol.* **56**, 199–208 (2019).
6. M. A. Tosches, From cell types to an integrated understanding of brain evolution: The case of the cerebral cortex. *Annu. Rev. Cell Dev. Biol.* **37**, 495–517 (2021).
7. L. Beaulieu-Laroche *et al.*, Enhanced dendritic compartmentalization in human cortical neurons. *Cell* **175**, 643–651 (2018).
8. S. J. Zottoli, D. S. Faber, The Mauthner cell: What has it taught us? *Neuroscientist* **6**, 26–38 (2000).
9. H. Korn, D. S. Faber, The Mauthner cell half a century later: A neurobiological model for decision-making? *Neuron* **47**, 13–28 (2005).
10. W. R. Jeffery, D. P. Martasian, Evolution of eye regression in the cavefish *Astyanax:* Apoptosis and the Pax-6 gene. *Am. Zool.* **38**, 685–696 (1998).
11. H. Wilkens, U. Strecker, Convergent evolution of the cavefish *Astyanax* (Characidae, Teleostei): Genetic evidence from reduced eye-size and pigmentation. *Biol. J. Linnean Soc.* **80**, 545–554 (2003).
12. M. Yoshizawa, S. Gorički, D. Soares, W. R. Jeffery, Evolution of a behavioral shift mediated by superficial neuromasts helps cavefish find food in the darkness. *Curr. Biol.* **20**, 1631–1636 (2010).
13. E. R. Duboué, A. C. Keene, R. L. Borowsky, Evolutionary convergence on sleep loss in cavefish populations. *Curr. Biol.* **21**, 671–676 (2011).
14. A. Beale *et al.*, Circadian rhythms in Mexican blind cavefish *Astyanax mexicanus* in the lab and in the field. *Nat. Commun.* **4**, 2769 (2013).
15. Y. Elipot, H. Hinaux, J. Callebert, S. Rétaux, Evolutionary shift from fighting to foraging in blind cavefish through changes in the serotonin network. *Curr. Biol.* **23**, 1–10 (2013).
16. S. Rétaux, D. Casane, Evolution of eye development in the darkness of caves: Adaptation, drift, or both? *EvoDevo* **4**, 26 (2013).
17. N. Rohner *et al.*, Cryptic variation in morphological evolution: HSP90 as a capacitor for loss of eyes in cavefish. *Science* **342**, 1372–1375 (2013).
18. S. Rétaux *et al.*, "Neural development and evolution in Astyanax mexicanus: Comparing cavefish and surface fish brains" in *Biology and Evolution of the Mexican Cavefish*, A. C. Keene, M. Yoshizawa, S. E. McGaugh, Eds. (Elsevier, 2016), pp. 227–244.
19. H. Wilkens, U. Strecker, *Evolution in the Dark* (Springer, 2017).
20. R. Borowsky, Cavefishes. *Curr. Biol.* **28**, R51–R65 (2018).
21. J. S. R. Chin *et al.*, Convergence on reduced stress behavior in the Mexican blind cavefish. *Dev. Biol.* **441**, 319–327 (2018).
22. E. Lloyd *et al.*, Evolutionary shift towards lateral line dependent prey capture behavior in the blind Mexican cavefish. *Dev. Biol.* **441**, 328–337 (2018).
23. M. R. Riddle *et al.*, Insulin resistance in cavefish as an adaptation to a nutrient-limited environment. *Nature* **555**, 647–651 (2018).
24. J. B. Jaggard *et al.*, Cavefish brain atlases reveal functional and anatomical convergence across independently evolved populations. *Sci. Adv.* **6**, eaba3126 (2020).
25. W. R. Jeffery, Astyanax surface and cave fish morphs. *EvoDevo* **11**, 14 (2020).
26. S. J. Zottoli, Correlation of the startle reflex and Mauthner cell auditory responses in unrestrained goldfish. *J. Exp. Biol.* **66**, 243–254 (1977).
27. A. Hecker, W. Schulze, J. Oster, D. O. Richter, S. Schuster, Removing a single neuron in a vertebrate brain forever abolishes an essential behavior. *Proc. Natl. Acad. Sci. U.S.A.* **117**, 3254–3260 (2020).
28. J. G. Canfield, G. J. Rose, Activation of Mauthner neurons during prey capture. *J. Comp. Physiol. A* **172**, 611–618 (1993).
29. S. Wöhl, S. Schuster, The predictive start of hunting archer fish: A flexible and precise motor pattern performed with the kinematics of an escape C-start. *J. Exp. Biol.* **210**, 311–324 (2007).
30. S. J. Zottoli, A. R. Hordes, D. S. Faber, Localization of optic tectal input to the ventral dendrite of the goldfish Mauthner cell. *Brain Res.* **401**, 113–121 (1987).
31. M. Mirjany, D. S. Faber, Characteristics of the anterior lateral line nerve input to the Mauthner cell. *J. Exp. Biol.* **214**, 3368–3377 (2011).
32. W. R. Elliott, "Cave biodiversity and ecology of the Sierra de El Abra region" in *Biology and Evolution of the Mexican Cavefish*, A. C. Keene, M. Yoshizawa, S. E. McGaugh, Eds. (Elsevier, 2016), pp. 59–75.

33. L. Espinasa *et al.*, Contrasting feeding habits of post-larval and adult *Astyanax* cavefish. *Subterranean Biol.* **21**, 1–17 (2017).
34. J. Coppola, L. Espinasa, Cave *Astyanax*: Hunters or scavengers? Evidence from gut contents. *Speleobiol. Notes* **10**, 28–37 (2019).
35. Z. Tanvir, D. Rivera, K. E. Severi, G. Haspel, D. Soares, Evolutionary and homeostatic changes in morphology of the visual dendrites of Mauthner cells in *Astyanax* blind cavefish. *J. Comp. Neurol.* **529**, 1779–1786 (2021).
36. D. S. Faber, H. Korn, "Electrophysiology of the Mauthner cell: Basic properties, synaptic mechanisms, and associated networks" in *Neurobiology of the Mauthner Cell*, D. S. Faber, H. Korn, Eds. (Raven Press, 1978), pp. 47–131.
37. H. S. Bierman, S. J. Zottoli, M. E. Hale, Evolution of the Mauthner axon cap. *Brain Behav. Evol.* **73**, 174–187 (2009).
38. E. J. Furshpan, T. Furukawa, Intracellular and extracellular responses of the several regions of the Mauthner cell of goldfish. *J. Neurophysiol.* **25**, 732–771 (1962).
39. D. S. Faber, J. R. Fetcho, H. Korn, Neuronal networks underlying the escape response in goldfish. *Ann. N.Y. Acad. Sci.* **563**, 11–33 (1989).
40. C. Hyacinthe, J. Attia, S. Rétaux, Evolution of acoustic communication in blind cavefish. *Nat. Commun.* **10**, 4231 (2019).
41. A. N. Popper, Auditory capacities of the Mexican blind cave fish (*Astyanax jordani*) and its eyed ancestor (*Astyanax mexicanus*). *Anim. Behav.* **18**, 552–562 (1970).
42. M. S. Enriquez *et al.*, Evidence for rapid divergence of sensory systems between Texas populations of the Mexican tetra (*Astyanax mexicanus*). *Front. Ecol. Evol.* **11**, 1085975 (2023).
43. R. C. Eaton, J. C. Hofve, J. R. Fetcho, Beating the competition: The reliability hypothesis for Mauthner axon size. *Brain Behav. Evol.* **45**, 183–194 (1995).
44. P. Machnik, K. Leupolz, S. Feyl, W. Schulze, S. Schuster, The Mauthner cell in fish with top-performance and yet flexibly tuned C-starts. II. Physiology. *J. Exp. Biol.* **221**, jeb175588 (2018).
45. T. Furukawa, E. J. Furshpan, Two inhibitory mechanisms in the Mauthner neurons of goldfish. *J. Neurophysiol.* **26**, 140–176 (1963).
46. E. Lloyd *et al.*, Blind cavefish retain functional connectivity in the tectum despite loss of retinal input. *Curr. Biol.* **32**, 3720–3730 (2022).
47. S. J. Zottoli, "Comparative morphology of the Mauthner cell in fish and amphibians" in *Neurobiology of the Mauthner Cell*, D. S. Faber, H. Korn, Eds. (Raven Press, 1978), pp. 13–45.
48. C. Smith, P. Reay, Cannibalism in teleost fish. *Rev. Fish Biol. Fish.* **1**, 41–64 (1991).
49. P. G. Jabłoński, N. J. Strausfeld, Exploitation of an ancient escape circuit by an Avian predator: Relationships between taxon-specific prey escape circuits and the sensitivity to visual cues from the predator. *Brain Behav. Evol.* **58**, 218–240 (2001).
50. M. J. Allen, T. A. Godenschwege, M. A. Tanouye, P. Phelan, Making an escape: Development and function of the *Drosophila* giant fibre system. *Semin. Cell Dev. Biol.* **17**, 31–41 (2006).
51. T. G. Langecker, H. Wilkens, P. Junge, Introgressive hybridization in the Pachon Cave population of *Astyanax fasciatus* (Teleostei: Characidae). *Ichthyol. Explor. Freshwaters* **2**, 209–212 (1991).
52. U. Strecker, V. H. Faúndez, H. Wilkens, Phylogeography of surface and cave *Astyanax* (Teleostei) from central and North America based on cytochrome *b* sequence data. *Mol. Phylogenet. Evol.* **33**, 469–481 (2004).
53. R. Borowsky, Selection maintains the phenotypic divergence of cave and surface fish. *Am. Nat.* **202**, 55–63 (2023).
54. P. Machnik, E. Schirmer, L. Glück, S. Schuster, Recordings in an integrating central neuron provide a quick way for identifying appropriate anaesthetic use in fish. *Sci. Rep.* **8**, 17541 (2018).
55. P. Machnik, K. Leupolz, S. Feyl, W. Schulze, S. Schuster, The Mauthner cell in fish with top-performance and yet flexibly tuned C-starts. I. Identification and comparative morphology. *J. Exp. Biol.* **221**, jeb182535 (2018).
56. M. Smith, A. E. Pereda, Chemical synaptic activity modulates nearby electrical synapses. *Proc. Natl. Acad. Sci. U.S.A.* **100**, 4849–4854 (2003).
57. Q. Huang, D. Zhou, M. DiFiglia, Neurobiotin™, a useful neuroanatomical tracer for in vivo anterograde, retrograde and transneuronal tract-tracing and for in vitro labeling of neurons. *J. Neurosci. Methods* **41**, 31–43 (1992).